

Nuclear Structure Calculations and Modern Nucleon-Nucleon Potentials

L. Coraggio,¹ A. Covello,¹ A. Gargano,¹ N. Itaco,¹ T. T. S. Kuo,² and R. Machleidt³

¹Dipartimento di Scienze Fisiche, Università di Napoli Federico II,
and Istituto Nazionale di Fisica Nucleare,
Complesso Universitario di Monte S. Angelo, Via Cintia - I-80126 Napoli, Italy

²Department of Physics, SUNY, Stony Brook, New York 11794

³Department of Physics, University of Idaho, Moscow, Idaho 83844

(Dated: April 16, 2024)

We study ground-state properties of the doubly magic nuclei ${}^4\text{He}$, ${}^{16}\text{O}$, and ${}^{40}\text{Ca}$ employing the Goldstone expansion and using as input four different high-quality nucleon-nucleon (NN) potentials. The short-range repulsion of these potentials is renormalized by constructing a smooth low-momentum potential $V_{\text{low } k}$. This is used directly in a Hartree-Fock approach and corrections up to third order in the Goldstone expansion are evaluated. Comparison of the results shows that they are only slightly dependent on the choice of the NN potential.

PACS numbers: 21.30.Fe, 21.60.Jz, 21.10.Dr

I. INTRODUCTION

In recent years, the study of the properties of nuclear systems starting from a free nucleon-nucleon (NN) potential V_{NN} has become a subject of special interest. This has been stimulated by the substantial progress made during the last decade in the development of NN potentials that reproduce with high precision the NN scattering data and deuteron properties [1, 2, 3, 4]. However, the fact that these potentials predict almost identical phase shifts does not imply, owing to their different on-shell behavior, that they should give the same results when employed in nuclear many-body calculations. It is therefore of great interest to investigate how much nuclear structure results depend on the NN potential one starts with, namely to try to assess the relevance of the on-shell effects in microscopic nuclear structure calculations.

The differences between various NN potentials in describing properties of nuclear matter have been investigated by several authors, the main aim being to try to assess the role of the various components of the nuclear force. In this context, we may mention the studies of Refs. [5, 6, 7, 8], where attention has been focused on modern phase-shift equivalent NN potentials.

As regards the study of finite nuclei, while a rather large number of realistic nuclear structure calculations have been carried out in the past few years, only a few attempts have been made [9, 10, 11] to study to which extent these calculations depend on the NN potential used as input. Actually, no detailed comparison of the results produced by different phase-shift equivalent potentials in the description of nuclear structure properties has yet been done. It may be worth mentioning, however, the work of Ref. [12], where different high-precision NN potentials have been considered to investigate the effects of nonlocalities on the triton binding energy.

On the above grounds, we have found it interesting and timely to perform nuclear structure calculations using different phase-shift equivalent NN potentials and

make a detailed comparison between the corresponding results. In a recent paper [13], we performed realistic calculations of the ground-state properties of some doubly magic nuclei within the framework of the Goldstone expansion approach, and showed that the rate of convergence is very satisfactory. Motivated by the results obtained in that work, in the present paper we make use of the Goldstone expansion to calculate the binding energies and rms charge radii of ${}^4\text{He}$, ${}^{16}\text{O}$, and ${}^{40}\text{Ca}$ for different phase-shift equivalent NN potentials. We feel that this is a good "laboratory" for a comparative study of the effects of NN potentials in finite nuclei. We consider the four high-quality NN potentials Nijmegen II [1], Argonne V18 [2], CD-Bonn [3], and N³LO [4].

As is well known, to perform nuclear structure calculations with realistic NN potentials one has to deal with the strong repulsive behavior of such potentials in the high-momentum regime. Recently, a new method to renormalize the bare NN interaction has been proposed [14, 15], which is proving to be an advantageous alternative to the use of the Brueckner G matrix [14, 16, 17, 18]. It consists in deriving from V_{NN} a low-momentum potential $V_{\text{low } k}$ defined within a cutoff momentum k . This is a smooth potential which preserves exactly the on-shell properties of the original V_{NN} and is suitable for being used directly in nuclear structure calculations.

As in our earlier work [13], we construct the $V_{\text{low } k}$ for each of the four above mentioned NN potentials. The various $V_{\text{low } k}$'s are then used directly in Hartree-Fock calculations. Once the self-consistent basis is obtained, we calculate the Goldstone expansion including diagrams up to third order in $V_{\text{low } k}$.

It is worth emphasizing that one of the main advantages of the $V_{\text{low } k}$ renormalization method, with respect to the G matrix one, is to preserve the phase-shift equivalence of the original NN potentials. Thus, it is particularly interesting to compare the results obtained in nuclear structure calculations employing on-shell equivalent $V_{\text{low } k}$'s.

The paper is organized as follows. In Sec. II we give a

brief description of the main features of the four phase-shift equivalent NN potentials considered in our study. In Sec. III we give an outline of the derivation of $V_{\text{low } k}$ and some details of our calculations. In Sec. IV we present and discuss our results. Some concluding remarks are given in Sec. V.

II. REALISTIC NUCLEON-NUCLEON POTENTIALS

As reported in the Introduction, we employ the Nijmegen II [1], Argonne V18 [2], CD-Bonn [3], and chiral $N^3\text{LO}$ [4] NN potentials, which have all been fitted to the Nijmegen phase-shift analysis as well as the proton-proton and neutron-proton data below 350 MeV [19]. It is well known that these potentials, even if they reproduce the NN data with almost the same accuracy, may have a rather different mathematical structure. The Nijmegen II and the Argonne V18 potentials are non-relativistic and defined in terms of local functions, which are multiplied by a set of spin, isospin and angular momentum operators. The CD-Bonn potential, based on relativistic meson field theory, is represented in terms of the covariant Feynman amplitudes for one-boson exchange, which are nonlocal [20]. The $N^3\text{LO}$ potential is based upon a chiral effective Lagrangian. The model includes one- and two-pion exchange contributions and so-called contact terms up to chiral order four, some of which are non-local.

All the above NN interactions reproduce equally well the same phase-shifts, so the corresponding on-shell matrix elements of the reaction matrix T are the same as well. However, this does not imply that the interactions are identical. The T -matrix is obtained from the Lippmann-Schwinger equation

$$T(k^0; k; k^2) = V_{NN}(k^0; k) + \int_0^1 P_0 \int_0^1 dq^2 dq V_{NN}(k^0; q) \frac{1}{k^2 - q^2} T(q; k; k^2); \quad (1)$$

where k , k^0 , and q stand for the relative momenta. Notice that the T -matrix is the sum of two terms, the Born term and an integral term. Notwithstanding the sum is the same, the individual terms may still be quite different. For example, in Fig. 1 we show the value of the 3S_1 T -matrix elements for $K_{\text{lab}} = 150$ MeV and $k = k^0 = k_0 = 1.34 \text{ fm}^{-1}$. They are indicated by the full circle and are practically identical for the four NN potentials we have employed. In Fig. 1 we display also the matrix elements $V_{NN}(k_0; k)$ as a function of k for the four potentials. The asterisks stand for the diagonal matrix elements $V_{NN}(k_0; k_0)$, which represent the Born approximation to T . From the inspection of this figure, it is clear that even if different V_{NN} 's reproduce the same

T -matrix element, the latter is obtained by summing two terms that are significantly different for each potential. More precisely, it is evident that Nijmegen II potential is a quite "hard" potential, its diagonal matrix element being very repulsive. So, in order to reproduce correctly the on-shell T -matrix element, it needs a large attractive contribution from the integral term of Eq. (1), the latter being related to the tensor component of the NN force and to its off-shell behavior (see Ref. [21] for a closer examination). On the other hand, the $N^3\text{LO}$ interaction is a rather "soft" potential, implying a smaller contribution from the integral term.

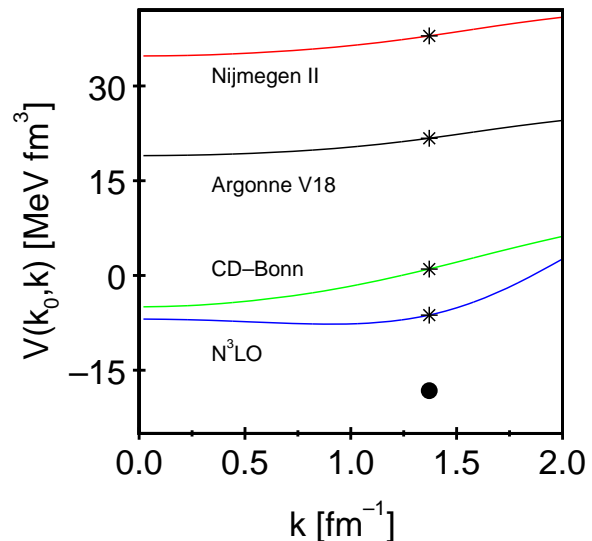


FIG. 1: Matrix elements $V_{NN}(k_0; k)$ for the 3S_1 partial wave for CD-Bonn (green line), Nijmegen II (red line), Argonne V18 (black line), and $N^3\text{LO}$ (blue line) potentials. The diagonal matrix elements $k_0 = 1.34 \text{ fm}^{-1}$ are marked by an asterisk. The corresponding T -matrix element is marked by a full circle (see text for more details).

Similar features may be observed also in the other partial waves, however, the differences among the potentials decrease for larger values of the orbital angular momentum.

III. METHOD OF CALCULATION

A traditional approach to the renormalization of the strong repulsive behavior of realistic NN potentials, when dealing with doubly closed-shell nuclei, is the Brueckner-Goldstone (BG) theory (see for instance Refs. [22, 23]), where the Goldstone perturbative expansion is re-ordered summing to all orders only the ladder diagrams. Consequently, the bare interaction (V_{NN}) vertices are replaced by the reaction matrix (G). This framework leads to the well known Brueckner-Hartree-Fock (BHF) theory, when the self-consistent definition is adopted for the single-particle (SP) auxiliary potential and only the first-order contribution in the BG expansion is taken into

account. So, the BHF approximation gives a mean field description of the ground state of nuclei in terms of the G matrix, the latter taking into account the correlations between pairs of nucleons. However this procedure is not without difficulties, because of the energy dependence of G.

As already mentioned in the Introduction, we renormalize the short-range repulsion of the bare NN potential by integrating out its high momentum components [14, 15]. The resulting low-momentum potential, $V_{\text{low } k}$, is a smooth potential, whose vertices can be used directly to sum up the Goldstone expansion diagrams.

According to the general definition of a renormalization group transformation, $V_{\text{low } k}$ must be such that the low-energy observables calculated in the full theory are preserved exactly by the effective theory.

For the nucleon-nucleon problem in vacuum, we require that the deuteron binding energy, low-energy phase shifts, and low-momentum half-on-shell T matrix calculated from V_{NN} must be reproduced by $V_{\text{low } k}$. The effective low-momentum T matrix is defined by

$$T_{\text{low } k}(p^0; p; p^2) = V_{\text{low } k}(p^0; p) + P \int_0^Z dq^2 dq V_{\text{low } k}(p^0; q) \frac{1}{p^2 - q^2} T_{\text{low } k}(q; p; p^2) : \quad (2)$$

Note that for $T_{\text{low } k}$ the intermediate states are integrated up to Z .

It is required that, for p and p^0 both belonging to $P(p; p^0)$, $T(p^0; p; p^2) = T_{\text{low } k}(p^0; p; p^2)$. In Refs. [14, 15] it has been shown that the above requirements are satisfied when $V_{\text{low } k}$ is given by the folded-diagram series

$$V_{\text{low } k} = \hat{Q} + \int_0^Z \hat{Q}^0 \hat{Q} + \int_0^Z \hat{Q}^0 \int_0^Z \hat{Q} + \dots ; \quad (3)$$

where \hat{Q} is an irreducible vertex function, in the sense that its intermediate states must be outside the model space P . The integral sign represents a generalized folding operation [24], and \hat{Q}^0 is obtained from \hat{Q} by removing terms of first order in the interaction.

The above $V_{\text{low } k}$ can be calculated by means of iterative techniques. We have used here an iteration method proposed in Ref. [25], which is particularly suitable for non-degenerate model spaces. This method, which we refer to as Andreozzi-Lee-Suzuki (ALS) method, is an iterative method of the Lee-Suzuki type [26].

To exemplify how $V_{\text{low } k}$ preserves low-energy observables, we report in Table I the deuteron binding energy, and the neutron-proton 1S_0 phase shifts calculated both

TABLE I: Deuteron binding energy (MeV) and $np \ ^1S_0$ phase shifts (deg) as predicted by full CD-Bonn and its $V_{\text{low } k}$ ($\Lambda = 2.0 \text{ fm}^{-1}$)

	CD-Bonn	$V_{\text{low } k}$	Expt.
B_d	2.224	2.224	2.224
Phase shifts			
E_{lab}			
1	62.1	62.1	62.1
10	60.0	60.0	60.0
25	50.9	50.9	50.9
50	40.5	40.5	40.5
100	26.4	26.4	26.8
150	16.3	16.3	16.9
200	8.3	8.3	8.9
250	1.6	1.6	2.0
300	-4.3	-4.3	-4.5

with the full CD-Bonn potential and its $V_{\text{low } k}$ (with a cut-off momentum $\Lambda = 2.0 \text{ fm}^{-1}$).

An important question in this approach is what value one should use for the cut-off momentum. A discussion of this point as well as a criterion for the choice of Λ can be found in Ref. [15]. According to this criterion, we have used here $\Lambda = 2.0 \text{ fm}^{-1}$.

After having renormalized the various NN potentials, we use the corresponding $V_{\text{low } k}$'s directly in a HF calculation. The HF equations are then solved for ^4He , ^{16}O and ^{40}Ca making use of a harmonic-oscillator (HO) basis. The details of the HF procedure are reported in Ref. [13]. As a major improvement, in this work we remove the spurious center-of-mass kinetic energy writing the kinetic energy operator T as

$$T = \frac{1}{2Am} \sum_{i < j}^X (p_i - p_j)^2 : \quad (4)$$

Similarly, we define the mean square radius operator as

$$r^2 = \frac{1}{A^2} \sum_{i < j}^X (r_i - r_j)^2 : \quad (5)$$

A complete review about center-of-mass correction in self-consistent theories may be found in Ref. [27]

In our calculations the HF-SP states are expanded in a finite series of $N = 5$ harmonic-oscillator wavefunctions for ^{16}O and ^{40}Ca , and $N = 6$ for ^4He . This truncation is sufficient to ensure that the HF results do not significantly depend on the variation of the oscillator constant $\sim!$, as we showed in Ref. [13]. The values of $\sim!$ adopted here have been derived from the expression $\sim! = 45A^{-1/3} - 25A^{-2/3}$ [28], which reproduces the rms radii in an independent-particle approximation with harmonic-oscillator wave functions. This expression gives $\sim! = 18, 14$ and 11 MeV for ^4He , ^{16}O and ^{40}Ca , respectively.

We use the HF basis to sum both the Goldstone expansion and the diagrams for the mean square charge radius $\langle r^2 \rangle$, including contributions up to third order in $V_{\text{low } k}$. Fig. 2 shows first-, second-, and third-order diagrams [29] of the Goldstone expansion.

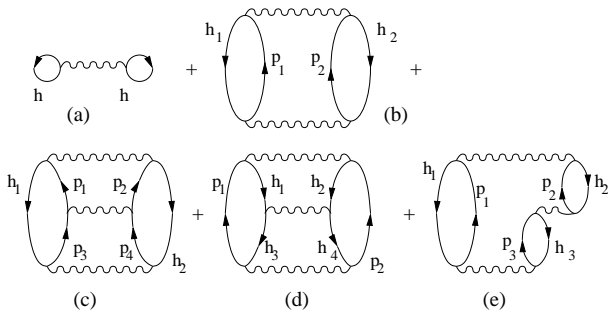


FIG. 2: First-, second-, and third-order diagrams in the Goldstone expansion.

IV. RESULTS

In Table II we show for ${}^4\text{He}$, ${}^{16}\text{O}$ and ${}^{40}\text{Ca}$ the calculated binding energy per nucleon and the rms charge radius obtained using different phase-shift equivalent NN potentials, and compare them with the experimental data [30, 31, 32].

TABLE II: Comparison of the calculated binding energies per nucleon (MeV/nucleon) and rms radii (fm) for different V_{NN} with the experimental data for ${}^4\text{He}$, ${}^{16}\text{O}$ and ${}^{40}\text{Ca}$. We take into account the finite dimensions of the proton using an estimate of its rms charge radius $r_p^2 = 0.8 \text{ fm}^2$ [31].

Nucleus		Nijmegen II	AV18	CD-Bonn	N ³ LO	Expt.
${}^4\text{He}$	BE/A	6.88	6.85	6.95	6.61	7.07
	$\langle r^2 \rangle^{i=2}$	1.68	1.69	1.63	1.75	1.67
${}^{16}\text{O}$	BE/A	8.26	8.26	8.30	8.11	7.98
	$\langle r^2 \rangle^{i=2}$	2.58	2.59	2.49	2.66	2.73
${}^{40}\text{Ca}$	BE/A	9.66	9.53	9.93	9.50	8.55
	$\langle r^2 \rangle^{i=2}$	3.20	3.22	3.10	3.29	3.485

A detailed analysis about the convergence properties of the perturbative series can be found in Ref. [13], where it is shown that the convergence is fairly rapid and higher-order contributions are negligible.

From Table II, we see that the calculated quantities are scarcely sensitive to the choice of the NN potential.

As a matter of fact, the binding energies per nucleon and the rms charge radii calculated using the various potentials differ at most by 0.43 MeV and 0.19 fm, respectively. This insensitivity may be traced back to the fact that when renormalizing the short-range repulsion of the

TABLE III: Calculated P_D 's with different NN potentials and with the corresponding $V_{\text{low } k}$'s

	Nijmegen II	AV18	CD-Bonn	N ³ LO
Full potential	5.63	5.76	4.85	4.51
$V_{\text{low } k}$	4.32	4.37	4.04	4.32

various potentials, the differences existing between their on-shell properties are attenuated. It is well known (see for instance [21]) that the on-shell behavior of a potential, and in particular its on-shell tensor force strength, is related to the D-state probability of the deuteron P_D ; this is why when comparing NN potentials, on-shell differences are seen in P_D differences. For this reason, we report in Table III the predicted P_D 's for each of the potentials under consideration, and compare them with those calculated with the corresponding $V_{\text{low } k}$'s. We see that while the P_D 's given by the full potentials are substantially different, ranging from 4.5 to 5.8%, they become quite similar after renormalization. This is an indication that the "on-shell equivalent" potentials we have used are made almost "on-shell equivalent" by the renormalization procedure. This aspect is more evident when comparing our calculated ${}^4\text{He}$ binding energies with the results of exact calculations, based on the Faddeev-Yakubovsky procedure [33, 34] (see Table IV). As a matter of fact, the difference between the exact results, that is at most 2 MeV, is reduced to 1.3 MeV in our calculations. It has to be observed that larger differences between our results and the exact ones are obtained when employing high- P_D potentials, such as Nijmegen II and Argonne V18. Smaller differences occur for the N³LO (1 MeV) and CD-Bonn (1.5 MeV) potentials, whose tensor force strengths are smaller than those of the two other potentials. This reflects the fact that for these two potentials the renormalization procedure modifies the original P_D to a limited extent, while a stronger change occurs for the Nijmegen II and Argonne V18 potentials. Table IV also shows that in all cases we get more binding than the exact calculations, as a consequence of the renormalization of the repulsive components of the potentials.

TABLE IV: Comparison of the ${}^4\text{He}$ calculated binding energies (MeV) for different V_{NN} obtained using Goldstone expansion (I) and with Faddeev-Yakubovsky procedure (II).

BE	Nijmegen II	AV18	CD-Bonn	N ³ LO
(I)	27.523	27.409	27.799	26.440
(II)	24.560	24.280	26.260	25.410

V. SUMMARY AND CONCLUSIONS

The aim of this work has been to compare the results of microscopic nuclear structure calculations, starting from

four different phase-shift equivalent NN potentials, Nijmegen II, Argonne V18, CD-Bonn, and N^3LO . To this end, we have calculated ground-state properties of the doubly closed nuclei 4He , ^{16}O , and ^{40}Ca by way of the Goldstone expansion. This has been done within the framework of the so-called $V_{low k}$ approach [14, 15] to the renormalization of the short-range repulsion of the NN potentials, wherein a low-momentum potential is derived, which preserves the low-energy physics of the original potential.

The analysis of the results obtained shows that the calculated properties are only weakly dependent on the NN potential used as input. This result may be traced back to the renormalization procedure of the short-range repulsion. As a matter of fact, we have shown that the renormalized potentials are characterized by a reduced o -shell tensor force strength, as compared with that of the original potential. Moreover, the P_D 's of the different potentials become quite similar, this quantity being related to the balance between the central and tensor

components of the nuclear force.

It is worthwhile to point out that when dealing with the N^3LO chiral potential, the renormalization procedure, which by construction preserves exactly the on-shell properties up to the cutoff momentum, scarcely modifies the o -shell behavior. This feature, which is related to the fact that chiral perturbation theory is a low-momentum expansion, may make this kind of NN potentials particularly tailored for microscopic nuclear structure calculations.

Acknowledgments

This work was supported in part by the Italian Ministero dell'Istruzione, dell'Università e della Ricerca (MIUR), by the U.S. DOE Grant No. DE-FG02-88ER40388, and by the U.S. NSF Grant No. PHY-0099444.

-
- [1] V.G.J. Stoks, R.A.M. Klomp, C.P.F. Terheggen, and J.J. de Swart, *Phys. Rev. C* **49**, 2950 (1994).
- [2] R.B. Wiringa, V.G.J. Stoks, and R. Schiavilla, *Phys. Rev. C* **51**, 38 (1995).
- [3] R. Machleidt, *Phys. Rev. C* **63**, 024001 (2001).
- [4] D.R. Entem and R. Machleidt, *Phys. Rev. C* **68**, 041001(R) (2003).
- [5] L. Engvik, M. Hjorth-Jensen, R. Machleidt, H. Muther, and A. Polls, *Nucl. Phys. A* **627**, 85 (1997).
- [6] M. Baldo, E. Ljajc, L. Engvik, M. Hjorth-Jensen, and H.-J. Schulze, *Phys. Rev. C* **58**, 1921 (1998).
- [7] H. Muther and A. Polls, *Phys. Rev. C* **61**, 014304 (1999).
- [8] T. Frick, K. Hagad, H. Muther, and P. Czerski, *Phys. Rev. C* **65**, 034321 (2002).
- [9] M.F. Jiang, R. Machleidt, D.B. Stout, and T.T.S. Kuo, *Phys. Rev. C* **46**, 910 (1992).
- [10] M. Hjorth-Jensen, T.T.S. Kuo, and E. Osnes, *Phys. Rep.* **261**, 125 (1995).
- [11] A. Covelto, L. Coraggio, A. Gargano, N. Itaco, and T.T.S. Kuo, *Proceedings of the Nuclear Structure 98 Conference, Gatlinburg, Tennessee, 1998*, edited by C. Baktash (AIP, New York, 1999).
- [12] R. Machleidt, F. Sammarruca, and Y. Song, *Phys. Rev. C* **53**, R1483 (1996).
- [13] L. Coraggio, N. Itaco, A. Covelto, A. Gargano, and T.T.S. Kuo, *Phys. Rev. C* **68**, 034320 (2003).
- [14] S. Bogner, T.T.S. Kuo and L. Coraggio, *Nucl. Phys. A* **684**, 432c (2001).
- [15] Scott Bogner, T.T.S. Kuo, L. Coraggio, A. Covelto, and N. Itaco, *Phys. Rev. C* **65**, 051301(R) (2002).
- [16] L. Coraggio, A. Covelto, A. Gargano, N. Itaco, and T.T.S. Kuo, *Phys. Rev. C* **66**, 064311 (2002).
- [17] L. Coraggio, A. Covelto, A. Gargano, N. Itaco, T.T.S. Kuo, D.R. Entem, and R. Machleidt, *Phys. Rev. C* **66**, 021303(R) (2002).
- [18] A. Covelto, L. Coraggio, A. Gargano, N. Itaco, and T.T.S. Kuo, in *Challenges of Nuclear Structure, Proceedings of the Eighth International Spring Seminar on Nuclear Physics, Maiori, Italy, 2001*, edited by A. Covelto (World Scientific, Singapore, 2002), p. 139.
- [19] V.G.J. Stoks, R.A.M. Klomp, M.C.M. Rentmeester, and J.J. de Swart, *Phys. Rev. C* **48**, 792 (1993).
- [20] R. Machleidt, *Adv. Nucl. Phys.* **19**, 189 (1989).
- [21] R. Machleidt and G.Q. Li, *Phys. Rep.* **242**, 5 (1994).
- [22] B.D. Day, *Rev. Mod. Phys.* **39**, 719 (1967).
- [23] I.S. Towner, *A Shell Model Description of Light Nuclei* (Clarendon Press, Oxford, 1977).
- [24] E.M. Kreniglowa and T.T.S. Kuo, *Nucl. Phys. A* **342**, 454 (1980).
- [25] F. Andreozzi, *Phys. Rev. C* **54**, 684 (1996).
- [26] K. Suzuki and S.Y. Lee, *Prog. Theor. Phys.* **64**, 2091 (1980).
- [27] K.T.R. Davies and Richard L. Becker, *Nucl. Phys. A* **176**, 1 (1971).
- [28] J. Blomqvist and A. Molinari, *Nucl. Phys. A* **106**, 545 (1968).
- [29] J. Goldstone, *Proc. Roy. Soc. (London)* **A 239**, 267 (1957).
- [30] G. Audi and A.H. Wapstra, *Nucl. Phys. A* **565**, 1 (1993).
- [31] H. de Vries, C.W. de Jager, and C. de Vries, *At. Data Nucl. Data Tables* **36**, 495 (1987).
- [32] E.G. Nadjakov, K.P. Marinova, and Yu.P. Gangrsky, *At. Data Nucl. Data Tables* **56**, 133 (1994).
- [33] A. Nogga, H. Kamada, and W. Glockle, *Phys. Rev. Lett.* **85**, 944 (2000).
- [34] P. Navrátil and E. Caurier, *Phys. Rev. C* **69**, 014311 (2004).